

University of Groningen

**A novel gamma-N-methylaminobutyrate demethylating oxidase involved in catabolism of the tobacco alkaloid nicotine by *Arthrobacter nicotinovorans* pAO1**

Chiribau, CB; Sandu, C; Fraaije, Marco; Schiltz, E; Brandsch, R; Chiribau, Calin B.

*Published in:*  
European Journal of Biochemistry

*DOI:*  
[10.1111/j.1432-1033.2004.04432.x](https://doi.org/10.1111/j.1432-1033.2004.04432.x)

**IMPORTANT NOTE: You are advised to consult the publisher's version (publisher's PDF) if you wish to cite from it. Please check the document version below.**

*Document Version*  
Publisher's PDF, also known as Version of record

*Publication date:*  
2004

[Link to publication in University of Groningen/UMCG research database](#)

*Citation for published version (APA):*

Chiribau, C. B., Sandu, C., Fraaije, M., Schiltz, E., Brandsch, R., & Chiribau, C. B. (2004). A novel gamma-N-methylaminobutyrate demethylating oxidase involved in catabolism of the tobacco alkaloid nicotine by *Arthrobacter nicotinovorans* pAO1. *European Journal of Biochemistry*, 271(23-24), 4677-4684. DOI: 10.1111/j.1432-1033.2004.04432.x

**Copyright**

Other than for strictly personal use, it is not permitted to download or to forward/distribute the text or part of it without the consent of the author(s) and/or copyright holder(s), unless the work is under an open content license (like Creative Commons).

**Take-down policy**

If you believe that this document breaches copyright please contact us providing details, and we will remove access to the work immediately and investigate your claim.

*Downloaded from the University of Groningen/UMCG research database (Pure): <http://www.rug.nl/research/portal>. For technical reasons the number of authors shown on this cover page is limited to 10 maximum.*

# A novel $\gamma$ -*N*-methylaminobutyrate demethylating oxidase involved in catabolism of the tobacco alkaloid nicotine by *Arthrobacter nicotinovorans* pAO1

Calin B. Chiribau<sup>1</sup>, Cristinel Sandu<sup>1</sup>, Marco Fraaije<sup>2</sup>, Emile Schiltz<sup>3</sup> and Roderich Brandsch<sup>1</sup>

<sup>1</sup>Institute of Biochemistry and Molecular Biology, University of Freiburg, Freiburg, Germany; <sup>2</sup>Laboratory of Biochemistry, University of Groningen, the Netherlands; <sup>3</sup>Institute of Organic Chemistry and Biochemistry, University of Freiburg, Freiburg, Germany

Nicotine catabolism, linked in *Arthrobacter nicotinovorans* to the presence of the megaplasmid pAO1, leads to the formation of  $\gamma$ -*N*-methylaminobutyrate from the pyrrolidine ring of the alkaloid. Until now the metabolic fate of  $\gamma$ -*N*-methylaminobutyrate has been unknown. pAO1 carries a cluster of ORFs with similarity to sarcosine and dimethylglycine dehydrogenases and oxidases, to the bifunctional enzyme methylenetetrahydrofolate dehydrogenase/cyclohydrolase and to formyltetrahydrofolate deformylase. We cloned and expressed the gene carrying the sarcosine dehydrogenase-like ORF and showed, by enzyme activity, spectrophotometric methods and identification of the reaction product as  $\gamma$ -aminobutyrate, that the predicted 89 395 Da flavoprotein is a demethylating  $\gamma$ -*N*-methylaminobutyrate oxidase. Site-directed mutagenesis identified His67 as the site

of covalent attachment of FAD and confirmed Trp66 as essential for FAD binding, for enzyme activity and for the spectral properties of the wild-type enzyme. A  $K_m$  of 140  $\mu$ M and a  $k_{cat}$  of 800 s<sup>-1</sup> was determined when  $\gamma$ -*N*-methylaminobutyrate was used as the substrate. Sarcosine was also turned over by the enzyme, but at a rate 200-fold slower than  $\gamma$ -*N*-methylaminobutyrate. This novel enzyme activity revealed that the first step in channelling the  $\gamma$ -*N*-methylaminobutyrate generated from nicotine into the cell metabolism proceeds by its oxidative demethylation.

**Keywords:** *Arthrobacter nicotinovorans*;  $\gamma$ -*N*-methylaminobutyrate oxidase; megaplasmid pAO1; nicotine degradation; sarcosine oxidase.

The bacterial soil community plays a pivotal role in the biodegradation of an almost unlimited spectrum of natural and man-made organic compounds, among them the tobacco alkaloid nicotine. Perhaps analysed in greatest detail is the pathway of nicotine degradation as it takes place in *Arthrobacter nicotinovorans* (formerly known as *A. oxydans*). Pioneering work on the identification of the enzymatic steps of this oxidative catabolic pathway was performed in the early 1960s by Karl Decker and co-workers at the University of Freiburg, Germany [1–8], and by Sidney C. Rittenberg and co-workers at the University of Southern California (Los Angeles, CA, USA) [9–14]. The first step in the breakdown of L-nicotine, the natural product synthesized by the tobacco plant, is the hydroxylation of the pyridine ring of nicotine in position six. This step is catalysed by nicotine dehydrogenase, a

heterotrimeric enzyme of the xanthine dehydrogenase family, which carries a molybdenum cofactor (MoCo), a FAD moiety and two iron-sulphur clusters [15,16]. Next, the pyrrolidine ring of 6-hydroxy-L-nicotine is oxidized by 6-hydroxy-L-nicotine oxidase [17]. A second hydroxylation of the pyridine ring of nicotine is performed by ketone dehydrogenase [18], an enzyme similar to nicotine dehydrogenase, yielding 2,6-dihydroxypseudooxynicotine [*N*-methylaminopropyl-(2,6-dihydroxypyridyl-3)-ketone] (Fig. 1). Cleavage of 2,6-dihydroxypseudooxynicotine by an as yet unknown enzyme, results in the formation of 2,6-dihydroxypyridine and  $\gamma$ -*N*-methylaminobutyrate [6,14]. 2,6-Dihydroxypyridine is hydroxylated to 2,3,6-trihydroxypyridine by the FAD-dependent 2,6-dihydroxypyridine hydroxylase [19] and, in the presence of O<sub>2</sub>, spontaneously forms a blue pigment, known as nicotine blue. The metabolic fate of  $\gamma$ -*N*-methylaminobutyrate was unknown until now.

Biodegradation of nicotine by *A. nicotinovorans* is linked to the presence of the megaplasmid, pAO1 [20]. The recent elucidation of the DNA sequence of pAO1 revealed the modular organization of the enzyme genes involved in nicotine degradation [21]. Next to a *nic*-gene cluster [19], there is a cluster of genes on pAO1 encoding the complete enzymatic pathway responsible for the synthesis of MoCo, required for enzyme activity by nicotine dehydrogenase and ketone dehydrogenase, and a gene cluster of an ABC molybdenum transporter. Adjacent to the *nic*-gene cluster is

Correspondence to R. Brandsch, Institut für Biochemie und Molekularbiologie, Hermann-Herder-Str. 7, 79104 Freiburg, Germany.

Fax: +49 761 2035253, Tel.: +49 761 2035231,

E-mail: roderich.brandsch@biochemie.uni-freiburg.de

Abbreviations: MABO,  $\gamma$ -*N*-methylaminobutyrate oxidase; MoCo, molybdenum cofactor.

Note: this article was dedicated to Karl Decker for the occasion of his 80th birthday.

(Received 2 September 2004, revised 7 October 2004, accepted 13 October 2004)

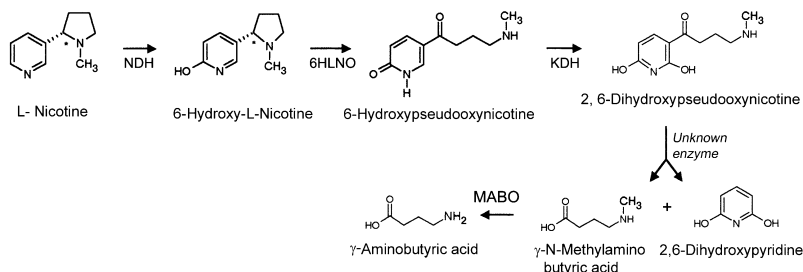


**Fig. 1.** Breakdown of nicotine by *Arthrobacter nicotinovorans* pAO1 (see the text for details). 6HLNO, 6-hydroxy-L-nicotine oxidase; KDH, ketone dehydrogenase; MABO,  $\gamma$ -N-methylaminobutyrate oxidase; NDH, nicotine dehydrogenase.

a set of hypothetical genes encoding a predicted flavo-enzyme similar to mitochondrial and bacterial sarcosine and dimethylglycine dehydrogenases and oxidases (ORF63), and two putative enzymes of tetrahydrofolate metabolism (ORF64 and ORF62) [21].

In the present work we show that the protein encoded by the sarcosine dehydrogenase-like ORF63 represents a novel enzyme, specific for the oxidative demethylation of  $\gamma$ -N-methylaminobutyrate generated from 2,6-dihydroxypseudooxynicotine. Identification of this enzyme extends our knowledge about the catabolic pathways of nicotine in bacteria and demonstrates that the first step in the metabolic turnover of  $\gamma$ -N-methylaminobutyrate consists of its demethylation.

## Experimental procedures

### Bacterial strains and growth conditions

*A. nicotinovorans* pAO1 was grown at 30 °C on citrate medium supplemented with vitamins, trace elements [22] and 5 mM of L-nicotine, as required. Growth of the culture was monitored by the increase in absorption at 600 nm. *Escherichia coli* XL1-Blue was employed as a host for plasmids and was cultured at 37 °C on LB (Luria–Bertani) medium, supplemented with the appropriate antibiotics.

### Cloning of the $\gamma$ -N-methylaminobutyrate oxidase (MABO) gene

pH6EX3 [23] is the expression vector used to clone the MABO gene. The DNA fragment carrying the MABO ORF was amplified with the primer pair 5'-GAC CTGAGTAGAAATGGATCCCTGATGGACAGG-3' and 5'-GGAATGGCTCGAGGGATCATCACC-3' bearing the restriction enzyme recognition sites *Bam*HI and *Xho*I, respectively. pAO1 DNA, isolated as described previously [20], was employed as a template in PCR amplifications performed as follows: 1 min at 95 °C, 40 s at 62 °C and 2 min at 72 °C, for 30 cycles, followed by one additional amplification round of 1 min at 95 °C, 40 s at 62 °C and 10 min at 72 °C. Pfu-Turbo high fidelity polymerase (Stratagene, Heidelberg, Germany) was used in the PCR. The amplified DNA fragment was ligated into pH6EX3 digested with the same restriction enzymes. *E. coli* XL1-Blue, made transformation competent with the Roti-Transform kit (Roth, Karlsruhe, Germany), were transformed with the ligated DNA and the bacteria were plated onto LB plates supplemented with 50  $\mu$ g·mL<sup>-1</sup> of ampicillin. Recombinant clones were verified by sequencing.

### Purification of MABO

The recombinant plasmid carrying the MABO gene was transformed into *E. coli* BL21 (Novagen, Schwalbach, Germany) and selected on 50  $\mu$ g·mL<sup>-1</sup> of ampicillin. One-hundred millilitres of LB medium was inoculated with a single colony, cultured overnight at 30 °C and used to inoculate 1 L of LB medium. MABO overexpression was induced with 0.3 mM isopropyl thio- $\beta$ -D-galactoside at 22 °C for 24 h. Bacteria were harvested at 5000 g, resuspended in 40 mM Hepes buffer, pH 7.4, containing 0.5 M NaCl, and disrupted with the aid of a Branson sonifier. The supernatant obtained by centrifugation of the bacterial lysate at 13 000 g was used to isolate the proteins on Ni-chelating Sepharose, as described by the supplier of the Sepharose (Amersham Biosciences, Freiburg, Germany). The isolated protein was analysed by SDS/PAGE on 10% (w/v) polyacrylamide gels. Superdex S-200 permeation chromatography, for determining the size of the native protein, was performed with the aid of a Mini-Maxi Ready Rack device, according to the suggestions of the supplier (Amersham Biosciences).

### Determination of enzyme activity

Enzyme activity was determined by using the peroxidase-coupled assay, consisting of 20 mM potassium phosphate buffer, pH 10, 25  $\mu$ M to 10 mM  $\gamma$ -aminobutyrate or 1–100 mM sarcosine as substrates, 10 IU·mL<sup>-1</sup> of horseradish peroxidase (Sigma, Steinheim, Germany), 0.007% (w/v) *o*-dianisidine (Sigma) and 10  $\mu$ g·mL<sup>-1</sup> of MABO. The reaction was initiated by the addition of substrate, and the increase in absorption at 430 nm caused by the oxidation of *o*-dianisidine was followed in an Ultrospec 3100 spectrophotometer (Amersham Biosciences). The pH optimum of the enzyme reaction was determined in potassium phosphate buffer of pH 5–10. A similar assay was employed in the activity staining of native MABO on nondenaturing polyacrylamide gels soaked in 10 mL of 20 mM potassium phosphate buffer, pH 10, containing 10 mM  $\gamma$ -N-methylaminobutyrate, 10 IU·mL<sup>-1</sup> of horseradish peroxidase, and 0.007% (w/v) *o*-dianisidine.

### TLC

Identification of the product of the reaction between  $\gamma$ -N-methylaminobutyrate and MABO was performed by TLC on Polygram Cel400 plates (Macherey-Nagel, Düren, Germany) with n-butanol/pyridine/acetic acid/H<sub>2</sub>O (10 : 15 : 3 : 12; v/v/v/v) as the mobile phase. One microlitre of a mix of 2 mM amino acids, consisting of

oxydized glutathione, lysine, alanine and leucine, and 1  $\mu$ L of a 10 mM solution of  $\gamma$ -aminobutyrate, were used as standards. The dry plates were developed by spraying with a 0.1% (v/v) ninydrine solution in acetone.

### State of FAD attachment to MABO

Noncovalent or covalent binding of FAD to MABO was determined by precipitation of the protein with trichloroacetic acid, and by the flavin fluorescence, in 10% (v/v) acetic acid, of the precipitated protein separated by SDS/PAGE on 10% (w/v) polyacrylamide gels.

### Site-directed mutagenesis of the *MABO* gene

The amino acid substitutions in the MABO protein were made with the aid of the Quick Change site-directed mutagenesis kit (Stratagene), according to the instructions of the supplier, and by using the primer pair 5'-GGCACCTCTTTGGGCCGCCGACAGGC-3' and 5'-GCC TGCGGCGGCCAAGAGGTGCC-3' for the H67A mutant, by using the primer pair 5'-GCAGCGGCAC CTCTTCTCACGCCGACAGGCTTG-3' and 5'-CAAG CCTGCGGCGTGAGAAGAGGTGCCGCTGC-3' for the W66S mutant, and by using the primer pair 5'-GCCACCTCTTTCCACGCCGACAGGC-3' and 5'-GC CTGCGGCGTGAAAGAGGTGCC-3' for the W66F mutant.

Spectroscopic measurements and determination of the FAD redox potential of MABO Spectra were recorded in a Lambda Bio40 UV/VIS spectrophotometer (PerkinElmer) or in an Ultrospec 3100 spectrophotometer (Amersham Biosciences). Reduction of the enzyme was accomplished by using  $\gamma$ -N-methylaminobutyrate, sarcosine and sodium dithionite under anaerobic conditions, achieved by flushing the cuvettes (Hellma, Müllheim, Germany) with high-quality nitrogen. In addition, reduction with substrates was performed in the presence of 1 U of glucose oxidase (Roche, Mannheim, Germany) and 1 mM glucose in order to deplete the oxygen from the assay. Sodium disulfite was used for sulfite titration experiments. Determination of the redox potential of MABO was performed as described previously [24], employing the xanthine/xanthine oxidase method.

### Western blotting of *A. nicotineovorans* pAO1 extracts

Purified MABO protein was used to raise an antiserum in rabbits according to standard protocols. Bacterial pellets from 1 L cultures of *A. nicotineovorans* pAO1, cultured as described above, were suspended in 5 mL of 0.1 M phosphate buffer, pH 7.4, containing 58 mM Na<sub>2</sub>HPO<sub>4</sub>, 17 mM NaH<sub>2</sub>PO<sub>4</sub>, 68 mM NaCl, 1 mM phenylmethylsulfonyl fluoride and 5 mg·mL<sup>-1</sup> lysozyme. After 1 h of incubation on ice, the bacterial suspensions were passed through a French pressure cell at 132 Mpa and the lysate was centrifuged for 30 min at 12 000 g. The extracts were analysed by SDS/PAGE on 10% (w/v) polyacrylamide gels and blotted onto nitrocellulose membranes (Optitran BA-S 85; Schleicher & Schuell, Dassel, Germany). The membranes were decorated with MABO antiserum and developed by using alkaline phosphatase-conjugated anti-rabbit IgG (Sigma) and Nitro Blue tetrazolium chloride as the indicator.

## Results

### ORF63 codes for a protein with covalently attached flavin, synthesized only in bacteria grown in the presence of nicotine

The DNA carrying the sarcosine dehydrogenase-like ORF63, corresponding to a protein of 813 amino acids with a predicted molecular mass of 89 395 kDa, was inserted into the expression vector pH6EX3, giving rise to a fusion protein with the N-terminal sequence MSPIHHHHHHLVPGSLM (one letter amino acid code; the underlined residue corresponds to the start methionine of ORF63). The protein was overexpressed in *E. coli* BL21, and the His-tagged protein was purified on Ni-chelating Sepharose. The purified protein analysed by SDS/PAGE on 10% (w/v) polyacrylamide gels showed a molecular mass of  $\approx$  90 000, in good agreement with the predicted size of the protein (Fig. 2A, lane 2 and lane 3). The protein isolated from *E. coli* BL-21 cultures grown at a temperature of  $>$  30 °C was practically colourless. However, when isolated from bacterial cultures grown at a temperature between 15 °C and 22 °C, the protein was yellow-coloured, typical of flavoenzymes. The trichloroacetic acid-precipitated protein retained its yellow colour and showed an intense fluorescence on SDS-polyacrylamide gels under UV light (Fig. 2A, lane 3). These features are characteristic of enzymes with a covalently attached flavin prosthetic group. The protein behaved on gel permeation chromatography (a Superdex 200 column) like a monomer with a molecular mass of  $\approx$  90 000 (data not shown).

When extracts of *A. nicotineovorans* pAO1, grown in the presence or absence of nicotine in the growth medium, were analysed by Western blotting for the presence of ORF63

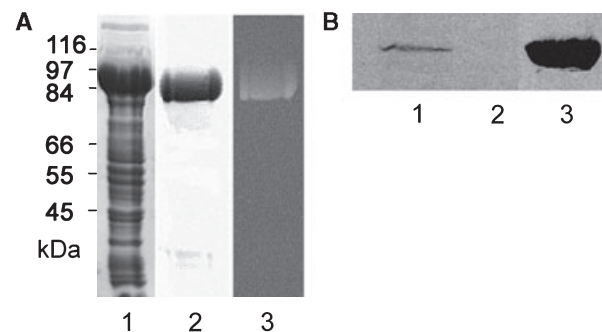


**Fig. 2. Purification, UV fluorescence and nicotine-dependent expression of the ORF63 protein.** (A) The H6-ORF63 protein was isolated by Ni-chelating chromatography from pH6EX3.*MABO* carrying *Escherichia coli* BL21 lysates, as described in the Experimental procedures and analysed by SDS/PAGE on 10% (w/v) polyacrylamide gels stained with Coomassie Brilliant Blue. Lane 1, 50  $\mu$ g of protein of *E. coli* lysate; lane 2, 10  $\mu$ g of purified H6-ORF63 protein; and lane 3, UV fluorescence of H6-ORF63 protein soaked in 10% acetic acid. To the left of the gel images are the molecular mass markers. (B) Expression of H6-ORF63 protein analysed by Western blotting of extracts of *Arthrobacter nicotineovorans* pAO1 grown in the presence (lane 1) and in the absence (lane 2) of nicotine, as described in the Experimental procedures. Lane 3, 1  $\mu$ g of purified H6-ORF63 protein as a control.

protein with specific antiserum, the protein was detected only in extracts of nicotine-grown bacteria (Fig. 2B, compare lane 1 with lane 2). The protein was not produced in a pAO1-deficient *A. nicotineovorans* strain, grown either in the presence or absence of nicotine (data not shown).

### The sarcosine dehydrogenase-like ORF63 protein is a $\gamma$ -*N*-methylaminobutyrate oxidase

Because the ORF63 protein was detected only in extracts of bacteria grown in the presence of nicotine, we reasoned that the hypothetical enzyme may be connected to nicotine catabolism. Cleavage of 2,6-dihydroxypseudooxynicotine yields  $\gamma$ -*N*-methylaminobutyrate, which would be a candidate substrate for an enzyme with similarity to sarcosine and dimethylglycine dehydrogenases and oxidases. Indeed, when the protein was tested on native polyacrylamide gels in a peroxidase-coupled assay with  $\gamma$ -*N*-methylaminobutyrate as the substrate, a characteristic colour developed at the position of the protein (Fig. 3A). The enzyme behaved like an oxidase and, with  $\gamma$ -*N*-methylaminobutyrate as the substrate, showed the kinetic parameters listed in Table 1. The pH optimum of the enzyme reaction was between pH 8 and pH 10. Sarcosine, but not dimethylglycine, was converted to a detectable extent (Table 1). Compounds structurally related to  $\gamma$ -*N*-methylaminobutyrate were not accepted as substrates (Table 1). Apparently, the enzyme is highly specific for  $\gamma$ -*N*-methylaminobutyrate, as the catalytic efficiency ( $k_{\text{cat}}/K_{\text{m}}$ ) with sarcosine is several orders of magnitude (36 000 $\times$ ) lower. Addition of tetrahydrofolate to the assay did not increase enzyme activity. As predicted, the

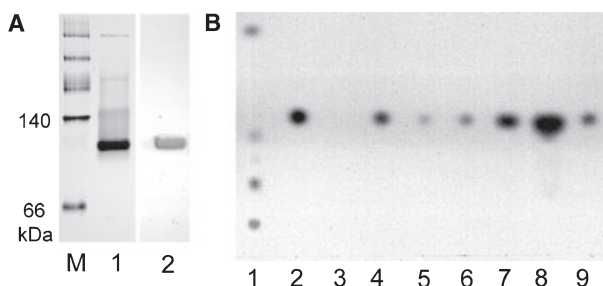
enzyme catalysed the demethylation of  $\gamma$ -*N*-methylaminobutyrate, yielding  $\gamma$ -aminobutyrate, as shown by TLC (Fig. 3B). Thus, the enzyme was found to be a demethylating  $\gamma$ -*N*-methylaminobutyrate oxidase (MABO). Cyclic compounds, such as L-proline, pipercolic acid or nicotine, were not turned over. *N*-Methylaminopropionate was, unfortunately, not at our disposition, but 2-methylaminoethanol was also no substrate and the carboxyl group of  $\gamma$ -*N*-methylaminobutyrate appeared to be important, as methylaminopropylamine and methylaminopropionitrile were not accepted by the enzyme. Compounds with long carbohydrate chains, such as 12-(methylamino)lauric acid [CH<sub>3</sub>-NH-(CH<sub>2</sub>)<sub>11</sub>-COOH], were not turned over.

### Flavin content and the UV-visible absorption spectrum of recombinant MABO

The UV-visible spectrum of MABO (Fig. 4A) exhibited absorption maxima centred at 278, 350 and 466 nm, with an additional shoulder at 500 nm. The ratio between the absorption at 280 nm and at 466 nm was 17.5 and this indicates a stoichiometry of 1 flavin molecule per protein molecule. Unfolding of the enzyme with SDS led to the disappearance of the shoulder at 500 nm and the formation of a spectrum typical for free flavin (Fig. 4A, dotted line). In contrast to flavoprotein dehydrogenases, flavoprotein oxidases typically react with sulfite to form a flavin N(5)-adduct [25,26]. MABO was found to react readily with sulfite, as the flavin spectrum was efficiently bleached by the addition of sulfite (Fig. 4C). Sulfite titration revealed effective formation of the flavin-sulfite adduct ( $K_{\text{D}} = 150 \mu\text{M}$ ). Anaerobic titration with  $\gamma$ -*N*-methylaminobutyrate and sarcosine resulted in full reduction of the enzyme without formation of flavin semiquinone species (Fig. 4B). This indicates that the enzyme is able to perform oxidation reactions which involve a 2-electron reduction of the flavin cofactor.

### Site-directed mutagenesis of MABO

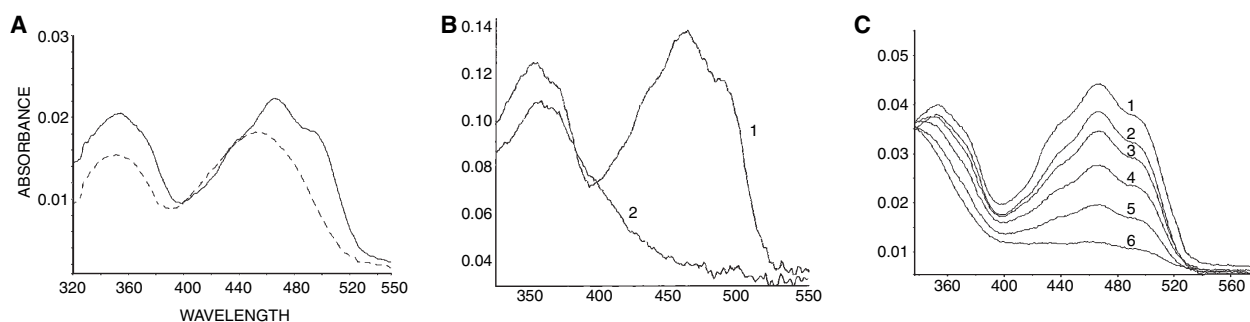
An amino acid alignment of the N-terminal sequence of pAO1 MABO, with the sequence of related enzymes, is shown in Fig. 5A. The alignment reveals, besides the characteristic dinucleotide-binding fingerprint amino acid motif, GXGXXG, a conserved His residue, typical for enzymes of this family. This His residue was first shown to be the site of covalent attachment of the FAD moiety in rat mitochondrial SaDH and DMGDH [27–30]. It is preceded in pAO1 MABO and in the mitochondrial enzymes by a Trp residue, which corresponds to a Ser residue in dimethylglycine oxidase from *Arthrobacter* spp. [31]. As expected from the alignment, replacement of His67 with Ala resulted in a protein without covalently bound flavin when tested by trichloroacetic acid precipitation and by UV fluorescence following SDS/PAGE (results not shown). The isolated protein contained noncovalently bound flavin and exhibited  $\approx 10\%$  of the enzyme activity of the wild-type enzyme. However, the UV-visible spectrum (Fig. 5B, dotted broken line, number 2) was very similar to that of the wild-type enzyme (Fig. 5B, continuous line, number 1), with a characteristic shift to higher wavelengths. Replacement of Trp66 by Ser also resulted in a noncovalently flavinylated



**Fig. 3. The ORF63 protein is a demethylating  $\gamma$ -*N*-methylaminobutyrate oxidase (MABO).** (A) MABO analysed by PAGE on nondenaturing 10% (w/v) polyacrylamide gels and stained with Coomassie brilliant blue (lane 1), or analysed by activity staining with  $\gamma$ -*N*-methylaminobutyrate as a substrate (lane 2), as described in the Experimental procedures. M, molecular mass markers. (B) Identification by TLC of  $\gamma$ -aminobutyrate as the reaction product of MABO. One microlitre of a 10 mM solution of  $\gamma$ -aminobutyrate (lanes 2 and 9); 1  $\mu\text{L}$  of a 10 mM solution of  $\gamma$ -*N*-methylaminobutyrate (lane 3, which does not react with the ninhydrine reagent); a mix of 1  $\mu\text{L}$  of  $\gamma$ -*N*-aminobutyrate and 1  $\mu\text{L}$  of  $\gamma$ -*N*-methylaminobutyrate (lane 4); 0.5  $\mu\text{L}$ , 1  $\mu\text{L}$ , 2  $\mu\text{L}$ , 5  $\mu\text{L}$  of a 1 mL enzyme assay with 10 mM  $\gamma$ -*N*-methylaminobutyrate as the substrate and 10  $\mu\text{g}$  of MABO incubated for 60 min (lanes 5–8) showing the formation of  $\gamma$ -*N*-aminobutyrate, were separated as described in the Experimental procedures on a TLC plate and developed with ninhydrine reagent. Lane 1, 1  $\mu\text{L}$  of a 2 mM amino acid mix (from bottom to top: oxidized glutathion, lysine, alanine and leucine) employed as a standard.

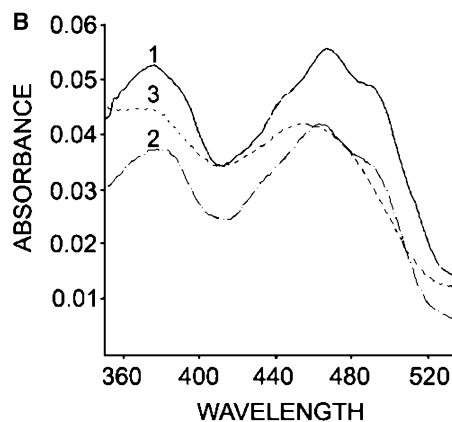
**Table 1.** Substrate specificity of  $\gamma$ -N-methylaminobutyrate oxidase (MABO).

Compound		$K_m$	$k_{cat}$ ( $s^{-1}$ )
$\gamma$ -Methylaminobutyrate	$CH_3-NH-(CH_2)_3-COOH$	140 $\mu M$	800
Sarcosine	$CH_3-NH-CH_2-COOH$	25 mM	4
Dimethylglycine	$CH_3-N-CH_2-COOH$	—	No substrate
	 CH <sub>3</sub>		
Methylaminopropionitrile	$CH_3-NH-(CH_2)_3-CN$	—	No substrate
Methylaminopropylamine	$CH_3-NH-(CH_2)_3-NH_2$	—	No substrate
$\alpha$ -Methylaminobutyrate	$CH_3-NH-CH-COOH$	—	No substrate
	 CH <sub>2</sub>		
	 CH <sub>3</sub>		

**Fig. 4.** UV-visible spectra of purified  $\gamma$ -N-methylaminobutyrate oxidase (MABO). (A) UV-visible spectra of MABO (—) and SDS unfolded MABO (- - -). (B) Anaerobic reduction of MABO with 10 mM  $\gamma$ -N-methylaminobutyrate: 1, oxidized spectrum; and 2, reduced spectrum. (C) Reaction of MABO with sodium disulfite (1, 0.005 mM; 2, 0.01 mM; 3, 0.05 mM; 4, 0.15 mM; 5, 0.5 mM; and 6, 5 mM sodium disulfite).

**A**

MABO	A.n.	11	<b>AS</b> MFTATSHD <b>PL</b> PTHV <b>RT</b> VV <b>GG</b> GIIGAS <b>I</b> AYHL <b>SA</b> AGEND <b>TL</b> LES <b>N</b> VLGS-- <b>GT</b> S <b>W</b> HAAG 70
SaDH	rat	53	<b>AS</b> VVPQ <b>Q</b> PS <b>Q</b> LP <b>LP</b> STAN <b>VV</b> IG <b>GG</b> SLG <b>Q</b> TYHLAKL <b>GV</b> GGV <b>V</b> LLERER <b>LT</b> S-- <b>GT</b> W <b>H</b> TAG 112
SaDH	R.l.	5	<b>I</b> PT <b>K</b> ARAV <b>I</b> IG <b>GG</b> VSG <b>CS</b> VAYHLAKL <b>GW</b> TD <b>I</b> V <b>LL</b> ER <b>K</b> Q <b>LT</b> S-- <b>GT</b> W <b>H</b> AA <b>G</b> 53
HDH	A.t.	1	<b>M</b> K <b>T</b> HARAV <b>V</b> IG <b>GG</b> V <b>GV</b> STLYHLAK <b>KG</b> WSD <b>SV</b> LLER <b>K</b> EL <b>T</b> S-- <b>G</b> ST <b>W</b> HAAG 50
DMGDH	rat	44	<b>E</b> T <b>V</b> IIG <b>GG</b> CV <b>GV</b> SLAYHLAK <b>AG</b> MRD <b>V</b> LL <b>E</b> K <b>S</b> EL <b>T</b> A-- <b>G</b> ST <b>W</b> HAAG 87
DMGO	A.g.	6	<b>R</b> V <b>I</b> I <b>G</b> AG <b>I</b> V <b>GT</b> N <b>L</b> ADEL <b>V</b> TR <b>GN</b> NI <b>T</b> VL <b>D</b> Q <b>GP</b> L <b>N</b> MP <b>GS</b> ST <b>S</b> H <b>A</b> PG 51

**Fig. 5.** Alignment of N-terminal amino acid sequences of selected enzymes related to pAO1  $\gamma$ -N-methylaminobutyrate oxidase (MABO) and UV-visible spectra of wild-type and mutant MABO proteins. (A) Amino acid alignment. Amino acids identical among MABO and one of the related enzymes are in bold type. The enzymes are rat mitochondrial sarcosine dehydrogenase (SaDH rat [29] Q88499, 30% identity with MABO), putative SaDH of *Rhizobium lotii* (SaDH R. l. Q98KW8, 41% identity with MABO), hypothetical dehydrogenase of *Agrobacterium tumefaciens* (HDH, Q8U599, 30% identity with MABO), rat dimethylglycine dehydrogenase (DMGDH rat [30], 30% identity with MABO), and dimethylglycine oxidase of *Arthrobacter globiformis* (DMGO A. g. [38] Q9AGP89, 30% identity with MABO). (B) UV-visible spectra: 1, continuous line, spectrum of wild-type MABO; 2, dotted broken line, spectrum of the H67A mutant; and 3, broken line, spectrum of the W66S mutant.



protein, but which was devoid of enzyme activity. The absorption spectrum of the mutant protein resembled the spectrum of free FAD, indicative of a significantly altered microenvironment around the isoalloxazine ring (Fig. 5B, broken line, number 3). Phe in place of Trp66 resulted in a protein with noncovalently bound FAD, again showing no enzyme activity, and isolation of the flavin cofactor from these mutant enzymes followed by TLC analysis showed it to be, as expected, FAD (not shown).

### Determination of the FAD redox potential of MABO

The xanthine/xanthine oxidase-mediated reduction of MABO gave rise to the formation of a one-electron-reduced flavin semiquinone anion with a typical absorbance maximum at 363 nm. The redox potential for the observed one-electron reduction could be determined by using 5,5-indigodisulfonate ( $E_m = -118$  mV) (Fig. 6) and was found to be  $-135$  mV. The  $\log(E_{ox}/E_{red})$  vs.  $\log(\text{dye}_{ox}/\text{dye}_{red})$  plots for the one-electron reduction gave a slope of 0.51. The red anionic flavin semiquinone was formed for more than 99% during the reaction, indicating that the redox potentials of the two couples (oxidized/semiquinone and semiquinone/hydroquinone) are separated by at least 200 mV [24,32]. The relatively low redox potential for the second 1-electron reduction could also be inferred from the fact that full reduction of the enzyme could not be established by using the xanthine oxidase method. While benzyl viologen ( $-359$  mV) and methyl viologen ( $E_m = -449$  mV) could be reduced in the presence of MABO, no significant reduction of the MABO semiquinone was observed. Apparently, the anionic semiquinone is strongly (kinetically) stabilized by the microenvironment of the flavin

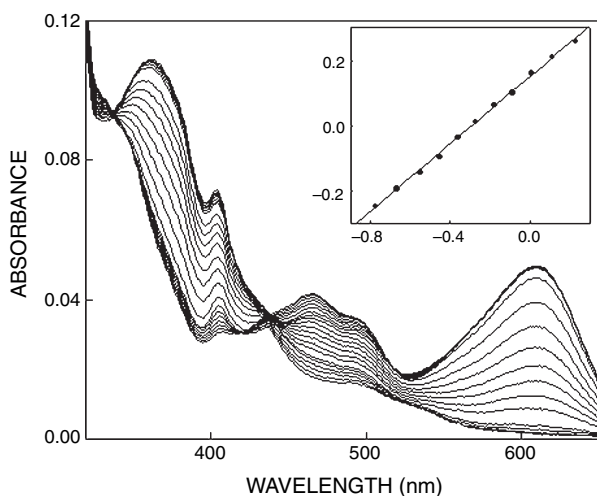


**Fig. 6.** Determination of the redox potential of wild-type  $\gamma$ -N-methylaminobutyrate oxidase (MABO). Selection of spectra obtained during reduction of  $6.25 \mu\text{M}$  MABO in HEPES buffer, pH 7.5, at  $25^\circ\text{C}$  in the presence of  $3 \mu\text{M}$  5,5-indigodisulfonate and  $2 \mu\text{M}$  methyl viologen. Reduction was accomplished by using the xanthine/xanthine oxidase method [24]. The reduction was complete after 90 min. The inset shows the  $\log(\text{MABO}_{ox}/\text{MABO}_{red})$  (measured at 467 nm) vs.  $\log(\text{dye}_{ox}/\text{dye}_{red})$  (measured at 612 nm) revealing a slope of 0.51, which is close to the theoretical value of 0.5.

cofactor. A similar redox behaviour was recently observed for glycine oxidase from *Bacillus subtilis* [25]. With the flavinylated mutants, again only the semiquinones could be formed during the redox titration. The corresponding redox potentials of the oxidized/semiquinone redox couples were found to be significantly lower compared to wild-type enzyme, as 5,5-indigodisulfonate was fully reduced before semiquinone was formed.

### Discussion

The pAO1 gene with similarity to mitochondrial and bacterial sarcosine and dimethylglycine dehydrogenases and oxidases was shown, in this work, to encode a demethylating oxidase with a novel substrate specificity. The enzyme efficiently converts  $\gamma$ -N-methylaminobutyrate, a compound generated during the catabolism of nicotine from 2,6-dihydroxypseudoxyxynicotine [6,14]. The enzyme demethylates  $\gamma$ -N-methylaminobutyrate, producing  $\gamma$ -aminobutyrate. The enzyme exhibited a narrow substrate specificity as, besides  $\gamma$ -N-methylaminobutyrate, only sarcosine was found to be converted to a detectable extent. The methyl group is probably transferred to tetrahydrofolate, the assumed second cofactor of the enzyme. Methylene-tetrahydrofolate may then be turned over by the bifunctional enzyme methylene-tetrahydrofolate dehydrogenase/cyclohydrolase and by formyl-tetrahydrofolate deformylase, the products of the two genes which form an operon with the gene of MABO (C. B. Chiribau & R. Brandsch, unpublished). The association of sarcosine oxidase genes with genes encoding enzymes of tetrahydrofolate-mediated C1 metabolism has been shown to be of general occurrence and has been described in detail for different bacteria [31,33]. The similarity of the C-terminal domain of MABO to other proteins of the sarcosine dehydrogenase and oxidase family may indicate that this is the site of attachment of tetrahydrofolate to the enzyme.  $\gamma$ -Aminobutyrate produced during the reaction may enter the general metabolism.

Compared to kinetic data from the literature obtained with the same peroxidase-coupled assay for tetrameric sarcosine oxidase ( $K_m = 3.4$  mM;  $k_{cat} = 5.8 \cdot \text{s}^{-1}$  [34]), monomeric sarcosine oxidase ( $K_m = 4.5$  mM;  $k_{cat} = 45.5 \cdot \text{s}^{-1}$  [35]) and dimethylglycine oxidase ( $K_m = 2$  mM;  $k_{cat} = 14.3 \cdot \text{s}^{-1}$  [31]), MABO with a  $K_m$  of 25 mM and a  $k_{cat}$  of  $4 \cdot \text{s}^{-1}$  and sarcosine as substrate is enzymatically less active. However, it is a catalytically highly efficient enzyme when  $\gamma$ -N-methylaminobutyrate is the substrate. This strongly supports the conclusion that  $\gamma$ -N-methylaminobutyrate is the natural substrate of the enzyme. The low  $K_m$  for  $\gamma$ -N-methylaminobutyrate may reflect the necessity of a high affinity for a substrate generated from L-nicotine present at low concentrations in the environment. The finding that MABO also exhibits sarcosine oxidase activity, may indicate an evolutionary relationship to sarcosine oxidases, enzymes largely distributed among soil bacteria. MABO may have evolved from a sarcosine oxidase by adjustment of the catalytic centre to accommodate the increased length of the carbohydrate chain.

MABO exhibits, like the mitochondrial sarcosine and dimethylglycine dehydrogenases [29,30], a tryptophan-histidine (WH) motif (see Fig. 5A), with His being the FAD attachment site. The H67A mutant contained, as expected,

a noncovalently bound FAD. The flavin absorbance maximum at lower wavelength was shifted dramatically (350 nm for the wild-type, 380 nm for the H67A mutant enzyme), which is indicative for breakage of the His–FAD bond [36]. However, loss of the covalent bond did not affect the spectral features of the absorbance maximum around 450 nm, an indication that binding and positioning of the flavin cofactor at the active site was not affected. Replacement of tryptophan with serine (W66S), also abolished covalent binding of FAD and resulted in an inactive enzyme variant. However, this inactivation was accompanied by a drastic change of the UV-visible spectrum. The observed unresolved absorbance maximum at 450 nm indicates that the flavin cofactor is bound in a different microenvironment from the wild-type enzyme, suggesting an important role for W66 in binding of the flavin cofactor. Tryptophan in this position also seems to be essential for covalent flavinylation as it could not be replaced without affecting covalent cofactor binding. As shown for other covalent flavo-proteins, covalent attachment of FAD can significantly alter the redox properties of the cofactor [36,37]. The wild-type enzyme was found to form and stabilize the red anionic flavin semiquinone, but could not be fully reduced using xanthine oxidase. The redox potential for the transfer of the first electron was found to be  $-135$  mV, while the redox potential for the second electron transfer is well below  $-449$  mV, resulting in a relatively low midpoint potential. As the redox potential for the second electron transfer could not be measured with the commonly used redox titration approach, the redox behaviour of the mutant enzymes were studied qualitatively. Again it was found that using the redox titration by xanthine oxidase only the semiquinone flavin could be formed. Interestingly, the redox potential for the first electron transfer of the mutant proteins was found to be significantly lower when compared with the wild-type enzyme, indicating that the mutation affects the redox behaviour of the flavin cofactor. The H67A mutant still exhibited  $\approx 10\%$  of the activity when compared with the wild-type enzyme. This is in line with a decreased redox potential, as a similar inactivating effect upon breaking the covalent cofactor-protein linkage has been observed with another oxidase. When breaking the histidyl–FAD bond in vanillyl-alcohol oxidase, a 10-fold inactivation was also observed, which could be correlated with a drop in redox potential [36].

During the course of this work, the structure of dimethylglycine oxidase from *A. globiformis* was published [38]. Examination of the structure shows that the serine side-chain, corresponding to W66 in MABO, does not belong to those residues making direct contact with the flavin. However, the conserved tryptophan may be important in positioning nearby active-site residues. Precise positioning of active-site residues is not only important for catalysing  $\gamma$ -N-methylaminobutyrate oxidation, but the covalent tethering of the flavin cofactor is an autocatalytic process [39] for which the active site has to be well defined [40].

The results of this work define a demethylating oxidase of novel substrate specificity, directed against  $\gamma$ -N-methylaminobutyrate, a compound generated during the catabolism of nicotine. The identification of this enzyme reveals, for the first time, the metabolic fate of the pyrrolidine ring of

nicotine during the pAO1-dependent nicotine catabolism by *A. nicotineovorans*.

## Acknowledgements

We wish to thank Carmen Brizio, Institute for Biochemistry and Molecular Biology, University of Bari, Italy, for fruitful discussions. This work was supported by a grant from the Graduiertenkolleg 434 of the Deutsche Forschungsgemeinschaft to R. B.

## References

1. Decker, K., Eberwein, H., Gries, F.A. & Brühmüller, M. (1960) Über den Abbau des Nicotins durch Bakterienenzyme. *Hoppe-Seyler's Z. Physiol. Chem.* **319**, 279–282.
2. Eberwein, H., Gries, F.A. & Decker, K. (1961) Über den Abbau des Nicotins durch Bakterienenzyme. II. Isolierung und Charakterisierung eines nicotinabbauenden Bodenbakteriums. *Hoppe-Seyler's Z. Physiol. Chem.* **323**, 236–248.
3. Decker, K., Gries, A. & Brühmüller, M. (1961) Über den Abbau des Nicotins durch Bakterienenzyme. III. Stoffwechselstudien an zellfreien Extrakten. *Hoppe-Seyler's Z. Physiol. Chem.* **323**, 249–263.
4. Decker, K., Eberwein, H., Gries, F.A. & Brühmüller, M. (1961) Über den Abbau des Nicotins durch Bakterienenzyme. IV. 1-6-Hydroxy-nicotine als erstes Zwischenprodukt. *Biochem. Z.* **334**, 227–244.
5. Gries, F.A., Decker, K. & Brühmüller, M. (1961) Über den Abbau des Nicotins durch Bakterienenzyme. V. Der Abbau des 1-6-hydroxy-nicotins zu [ $\gamma$ -methylamino-propyl]-[6-hydroxy-pyridyl-(3)]-ketons. *Hoppe-Seyler's Z. Physiol. Chem.* **325**, 229–241.
6. Gries, F.A., Decker, K., Eberwein, H. & Brühmüller, M. (1961) Über den Abbau des Nicotins durch Bakterienenzyme. VI. Die enzymatische Umwandlung des [ $\gamma$ -methylamino-propyl]-[6-hydroxy-pyridyl-(3)]-ketons. *Biochem. Z.* **335**, 285–302.
7. Decker, K. & Bleeg, H. (1965) Induction and purification of stereospecific nicotine oxidizing enzymes from *Arthrobacter oxidans*. *Biochem. Biophys. Acta* **105**, 313–334.
8. Gloger, M. & Decker, K. (1969) Zum Mechanismus der Induktion nicotinabbauender Enzyme in *Arthrobacter oxydans*. *Z. Naturforsch.* **24b**, 1016–1025.
9. Hochstein, L.I. & Rittenberg, S.C. (1958) The bacterial oxidation of nicotine. I. Nicotine oxidation by cell-free preparations. *J. Biol. Chem.* **234**, 151–155.
10. Hochstein, L.I. & Rittenberg, S.C. (1959) The bacterial oxidation of nicotine. II. The isolation of the first product and its identification as (1)-6-hydroxynicotine. *J. Biol. Chem.* **234**, 156–162.
11. Hochstein, L.I. & Rittenberg, S.C. (1960) The bacterial oxidation of nicotine. III. The isolation and identification of 6-hydroxypseudooxynicotine. *J. Biol. Chem.* **235**, 795–799.
12. Richardson, S.H. & Rittenberg, S.C. (1961) The bacterial oxidation of nicotine. IV. The isolation and identification of 2,6-dihydroxy-N-methylmyosmine. *J. Biol. Chem.* **236**, 959–963.
13. Richardson, S.H. & Rittenberg, S.C. (1961) The bacterial oxidation of nicotine. V. Identification of 2,6-dihydroxypseudooxynicotine as the third oxidation product. *J. Biol. Chem.* **236**, 964–967.
14. Gherna, R.L., Richardson, S.H. & Rittenberg, S.C. (1965) The bacterial oxidation of nicotine. VI. The metabolism of 2,6-dihydroxypseudooxynicotine. *J. Biol. Chem.* **240**, 3669–3674.
15. Freudenberg, W., König, K. & Andreesen, J.R. (1988) Nicotine dehydrogenase from *Arthrobacter oxydans*: a molybdenum-containing hydroxylase. *FEMS Microbiol. Lett.* **52**, 13–18.
16. Grether-Beck, S., Igloi, G.L., Pust, S., Schiltz, E., Decker, K. & Brandsch, R. (1994) Structural analysis and molybdenum-dependent expression of the pAO1-encoded nicotine dehydrogenase genes of *Arthrobacter nicotineovorans*. *Mol. Microbiol.* **13**, 929–936.



17. Dai, V.D., Decker, K. & Sund, H. (1968) Purification and properties of L-6-hydroxynicotine oxidase. *Eur. J. Biochem.* **4**, 95–102.
18. Schenk, S., Hoelz, A., Krauß, B. & Decker, K. (1998) Gene structure and properties of enzymes of the plasmid-encoded nicotine catabolism of *Arthrobacter nicotinovorans*. *J. Mol. Biol.* **284**, 1322–1339.
19. Baitsch, D., Sandu C. & Brandsch R. (2001) A gene cluster on pAO1 of *Arthrobacter nicotinovorans* involved in the degradation of the plant alkaloid nicotine: cloning, purification and characterization of 2,6-dihydroxypyridine 3-hydroxylase. *J. Bacteriol.* **183**, 5262–5267.
20. Brandsch, R. & Decker, K. (1984) Isolation and partial characterisation of plasmid DNA from *Arthrobacter oxydans*. *Arch. Microbiol.* **138**, 15–17.
21. Igloi, G.L. & Brandsch, R. (2003) Sequence of the 165-kilobase catabolic plasmid pAO1 from *Arthrobacter nicotinovorans* and identification of a pAO1-dependent nicotine uptake system. *J. Bacteriol.* **185**, 1976–1986.
22. Brühmüller, M., Schimz, A., Messmer, L. & Decker, K. (1975) Covalently bound FAD in D-6-hydroxynicotine oxidase. *J. Biol. Chem.* **250**, 7747–7751.
23. Berthold, H., Scanarini, M., Abney, C.C., Frorath, B. & Northemann, W. (1992) Purification of recombinant antigenic epitopes of the human 68-kDa (U1) ribonucleoprotein antigen using the expression system pH6EX3 followed by metal chelating affinity chromatography. *Protein Expr. Purif.* **3**, 50–56.
24. Massey, V. (1991) A simple method for the determination of redox potentials. In *Flavins and Flavoproteins 1990* (Curti, B., Ronchi, S. & Zanetti, G., eds), pp. 59–66. Walter de Gruyter, New York.
25. Job, V., Marcone, G.L., Pilone, M.S. & Pollegioni, L. (2002) Glycine oxidase from *Bacillus subtilis*. Characterization of a new flavoprotein. *J. Biol. Chem.* **277**, 6985–6993.
26. Massey, V., Müller, F., Feldberg, R., Schuman, M., Sullivan, P.A., Howell, L.G., Mayhew, S.G., Matthews, R.G. & Foust, G.P. (1969) The reactivity of flavoproteins with sulfite. Possible relevance to the problem of oxygen reactivity. *J. Biol. Chem.* **244**, 3999–4006.
27. Porter, D.H., Cook, R.J. & Wagner, C. (1985) Enzyme properties of dimethylglycine dehydrogenase and sarcosine dehydrogenase from rat liver. *Arch. Biochem. Biophys.* **243**, 396–407.
28. Cook, R.J., Misono, K.S. & Wagner, C. (1984) Identification of the covalently bound flavin of dimethylglycine dehydrogenase and sarcosine dehydrogenase from rat liver. *J. Biol. Chem.* **259**, 12475–12480.
29. Bergeron, F., Otto, A., Blache, P., Day, R., Denoroy, L., Brandsch, R. & Bataile, D. (1998) Molecular cloning and tissue distribution of rat sarcosine dehydrogenase. *Eur. J. Biochem.* **257**, 556–561.
30. Lang, H., Polster, M. & Brandsch, R. (1991) Dimethylglycine dehydrogenase from rat liver: characterization of a cDNA clone and covalent labeling of the polypeptide with <sup>14</sup>C-FAD. *Eur. J. Biochem.* **198**, 793–799.
31. Meskys, R., Harris, R.J., Casaitė, V., Basran, J. & Scrutton, N.S. (2001) Organization of the genes involved in dimethylglycine and sarcosine degradation in *Arthrobacter* spp. implications for glycine betaine catabolism. *Eur. J. Biochem.* **268**, 3390–3398.
32. Minnaert, K. (1965) Measurement of the equilibrium constant of the reaction between cytochrome *c* and cytochrome *a*. *Biochim. Biophys. Acta* **110**, 42–56.
33. Chlumsky, L.J., Zhang, L. & Jorns, M.S. (1995) Sequence analysis of sarcosine oxidase and nearby genes reveals homologies with key enzymes of folate one-carbon metabolism. *J. Biol. Chem.* **270**, 18252–18259.
34. Suzuki, M. (1981) Purification and some properties of sarcosine oxidase from *Corynebacterium* sp. U-96. *J. Biochem.* **89**, 599–607.
35. Wagner, M.A. & Jorns, M.S. (2000) Monomeric sarcosine oxidase: 2. Kinetic studies with sarcosine, alternate substrates and a substrate analogue. *Biochemistry* **39**, 8825–8829.
36. Fraaije, M.W., van den Heuvel, R.H.H., van Berkel, W.J.H. & Mattevi, A. (1999) Covalent flavinylation is essential for efficient redox catalysis in vanillyl-alcohol oxidase. *J. Biol. Chem.* **274**, 35514–35520.
37. Blaut, M., Whittaker, K., Valdovinos, A., Ackrell, B.A.C., Gunsalus, R.P. & Cecchini, G. (1989) Fumarate reductase mutants of *Escherichia coli* that lack covalently bound flavin. *J. Biol. Chem.* **264**, 13599–13604.
38. Leys, D., Basran, J. & Scrutton, N.S. (2003) Channeling and formation of 'active' formaldehyde in dimethylglycine oxidase. *EMBO J.* **22**, 4038–4048.
39. Brandsch, R. & Bichler, V. (1991) Autoflavinylation of apo-6-hydroxy-D-nicotine oxidase. *J. Biol. Chem.* **266**, 19056–19062.
40. Fraaije, M.W., Den Heuvel, R.H.H., van Berkel, W.J.H. & Mattevi, A. (2000) Structural analysis of flavinylation in vanillyl-alcohol oxidase. *J. Biol. Chem.* **275**, 38654–38658.